The FEBS Journal

FEBS PRESS science publishing by scientists

A new cryptic cationic antimicrobial peptide from human apolipoprotein E with antibacterial activity and immunomodulatory effects on human cells

Katia Pane[1,2,#], Valeria Sgambati[1,#], Anna Zanfardino[1], Giovanni Smaldone[3], Valeria Cafaro[1], Tiziana Angrisano[1], Emilia Pedone[4], Sonia Di Gaetano[4], Domenica Capasso[5], Evan F. Haney[2], Viviana Izzo[6], Mario Varcamonti[1], Eugenio Notomista[1], Robert E.W. Hancock[2], Alberto Di Donato[1] and Elio Pizzo[1]

1 Department of Biology, University of Naples Federico II, Naples, Italy
2 Department of Microbiology and Immunology, Centre for Microbial Diseases and Immunity Research, University of British Columbia, Vancouver, BC, Canada
3 IRCCS SDN, Naples, Italy
4 Institute of Biostructures and Bioimaging, C.N.R., Naples, Italy
5 Department of Pharmacy, University of Naples Federico II, Naples, Italy
6 Department of Medicine and Surgery, University of Salerno, Baronissi (SA), Italy

Keywords
antimicrobial peptides; apolipoprotein E; immunomodulation; inflammation; lipopolysaccharide

Correspondence
E. Pizzo, Department of Biology, University of Naples Federico II, Via Cintia, 80126, Naples, Italy
Fax: +39 081679233
Tel:+39 081679151
E-mail: elipizzo@unina.it

[#]Contributed equally.

(Received 24 November 2015, revised 28 February 2016, accepted 29 March 2016)

doi:10.1111/febs.13725

Cationic antimicrobial peptides (AMPs) possess fast and broad-spectrum activity against both Gram-negative and Gram-positive bacteria, as well as fungi. It has become increasingly evident that many AMPs, including those that derive from fragments of host proteins, are multifunctional and able to mediate various immunomodulatory functions and angiogenesis. Among these, synthetic apolipoprotein-derived peptides are safe and well tolerated in humans and have emerged as promising candidates in the treatment of various inflammatory conditions. Here, we report the characterization of a new AMP corresponding to residues 133–150 of human apolipoprotein E. Our results show that this peptide, produced either by chemical synthesis or by recombinant techniques in *Escherichia coli*, possesses a broad-spectrum antibacterial activity. As shown for several other AMPs, ApoE (133–150) is structured in the presence of TFE and of membrane-mimicking agents, like SDS, or bacterial surface lipopolysaccharide (LPS), and an anionic polysaccharide, alginate, which mimics anionic capsular exo-polysaccharides of several pathogenic microorganisms. Noteworthy, ApoE (133–150) is not toxic toward several human cell lines and triggers a significant innate immune response, assessed either as decreased expression levels of proinflammatory cytokines in differentiated THP-1 monocytic cells or by the induction of chemokines released from PBMCs. This novel bioactive AMP also showed a significant anti-inflammatory effect on human keratinocytes, suggesting its potential use as a model for designing new immunomodulatory therapeutics.

Abbreviations
AMP, antimicrobial peptide; CaCo-2, human epithelial colorectal adenocarcinoma cells; CD, circular dichroism; CFU, colony-forming units; Cox-2, cyclooxygenase-2; ELISA, enzyme-linked immunosorbent assay; FBS, fetal bovine serum; Fmoc, 9- fluorenylmethoxy carbonyl; HaCat, immortalized aneuploidy human keratinocyte cell line; HEK, human embryonic kidney 293 cell line; HeLa, human cervical carcinoma cell line; HPLC, high-performance (pressure) liquid chromatography; IDR, innate defense regulator; IL-8, interleukin-8; LB, Luria–Bertani; LPS, lipopolysaccharide; MCP-1, monocyte chemoattractant protein-1; MDR, multidrug resistance; MIC, minimum inhibitory concentration; MTT, 3-(4,5-dimethylthiazol-2-yl)-2,5-diphenyl tetrazolium; NB, nutrient broth; O.D., optical density; PBMCs, peripheral blood mononuclear cells; PMA, phorbol 12- myristate 13-acetate; TFE, 2,2,2-trifluoroethanol; THP-1, human monocytic cell line; TNF-α, tumor necrosis factor α; TSB, tryptic soy broth.

Introduction

Cationic antimicrobial peptides (AMPs) are essential components of the innate immune response of multicellular eukaryotes [1,2]. They are small cationic peptides characterized by an abundance of hydrophobic and positively charged amino acids. The net positive charge causes their adsorption at the surface of bacterial membranes that are rich in negatively charged lipids [3], allowing their translocation across the cytoplasmic membrane. This may lead either to membrane permeabilization, interfering with membrane associated enzymes involved in essential processes such as cell wall synthesis, or to attack intracellular targets and/ or macromolecular synthesis, eventually leading to cell death [2]. In contrast, AMPs are not as efficiently adsorbed at the surface of eukaryotic membranes that largely possess zwitterionic lipids on their surface [4] but are often able to translocate across the cytosolic membrane [1]. Several AMPs are already in clinical or preclinical trials for topical treatments [1,5].

In addition to their direct antibacterial activity, many AMPs often possess immunomodulatory activities such as chemokine induction and inhibition of lipopolysaccharide (LPS)-induced proinflammatory cytokine production. Additionally, some AMPs have been shown to stimulate angiogenesis, promote differentiation of immune cells, provide immune-based anti-infective activity in animal models and possess wound healing activity [1].

In multicellular eukaryotes, several proteins, with functions that are not necessarily related to host defense, have been discovered to act as sources of 'cryptic' AMPs, including hemoglobin, thrombin, lactoferrin, lysozyme, histone-like proteins, ribonucleases, and apolipoproteins [6–8]. These proteins, known as AMP-releasing proteins, release biologically active peptides only after proteolytic processing by bacterial and/or host proteases.

Apolipoprotein E (ApoE) is a well-known glycosylated protein that plays a key role in the transport of cholesterol and other lipids in the blood and central nervous system. ApoE is predominantly synthesized in the liver but it is also found in the brain, spleen, lungs, kidneys, ovaries, testes, peripheral nerves, and muscular tissues [9]. In addition to its role in lipid transport, several studies have shown its importance in the pathogenesis of atherosclerosis [10], neurodegenerative disorders such as Alzheimer's and Parkinson's disease [11], and autoimmune disorders such as multiple sclerosis [12] and psoriasis [13].

In addition to these well-established roles, ApoE also has immunomodulatory properties. Indeed, it has been observed that ApoE is able to induce an anti-inflammatory phenotype in macrophages [14], suppress proliferation of T cells [15,16], up-regulate the production of nitric oxide in platelets [17], and facilitate the presentation of lipid antigen by CD1 molecules on natural killer T cells [18]. These immunomodulatory properties appear to be biologically relevant, as ApoE-deficient animals have impaired immunity after exposure to *Listeria monocytogenes* and are more susceptible to endotoxemia after inoculation with LPS or *Klebsiella pneumoniae* [19,20]. These observations suggest that ApoE has important biological functions, independent from its canonical role in hepatic and peripheral tissue binding of cholesterol-rich lipoproteins.

A variety of enzymes, such as cathepsin D, thrombin, chymotrypsin-like serine protease, and aspartic proteases, have been proposed to mediate ApoE cleavage [21]. Fragments of ApoE have been detected in the brain and cerebrospinal fluid of Alzheimer's disease patients and have been shown to cause neurotoxicity under a variety of experimental conditions [22]. Moreover, studies carried out on synthetic peptides derived from the full-length protein have revealed neurotoxic effects similar to that of the intact protein, in addition to various other biological functions, including antimicrobial and immunomodulatory properties [23,24].

Several studies on ApoE have focused on the receptor-binding region [25–27], which is located between residues 130–162 (Fig. 1A) and is critical for its biological activities. The crystal structure of ApoE shows that this region folds into a long and amphipatic α-helix (Fig. 1B) that is part of a four-helix bundle (residues 24–167) that characterizes the fold of the N-terminal domain [28–30]. Interestingly, some studies have demonstrated that synthetic peptides covering the ApoE receptor-binding region retain the biological activities of the intact protein. For example, synthetic peptide Ac-ApoE (133–149)-NH_2, also known as 'COG-133' (see Fig. 1C), shows several interesting pharmacological characteristics such as anti-inflammatory and neuroprotective activity [31,32]. The cytostatic and cytotoxic effects of a panel of monomeric and dimeric synthetic peptides encompassing amino acids 130–169 of ApoE on IL2-dependent T lymphocytes have also been studied [25] revealing the importance of a high α-helical content in the ApoE-derived peptides and the key contribution of positively charged amino acids in the region 141–149.

A number of studies have focused on antimicrobial peptides derived from fragments of ApoE. Azuma and coworkers demonstrated that a peptide corresponding to residues 133–162 had a broad-spectrum antimicrobial activity [33]. In the same region, Forbes and

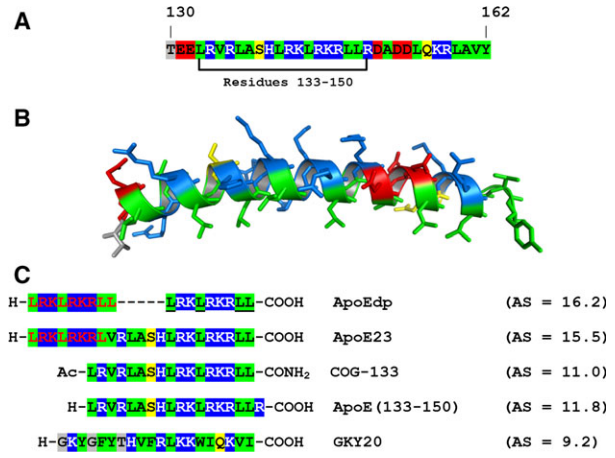

Fig. 1. Analysis of the apolipoprotein E region 130–162. Panel A shows the sequence of apolipoprotein E region 130–162 colored according to the properties of amino acids. Residues 133–150 are underlined. Panel B shows the structure of the region 130–162 (PDB code: 1B68). Panel C compares the sequences of the apolipoprotein E-derived peptides and the sequence of GKY20; the peptide identified in the C-terminal region of human thrombin heavy chain and used as control in the present work. Duplicated regions in ApoEdp and ApoE23 are shown in red. For each peptide, the calculated antimicrobial score (AS) is shown on the right (details on the meaning of AS can be found in the Introduction). In all the panels, the same color code was used: red, acidic residues (D, E); green, hydrophobic residues (L,I,V,A,M,W,F,Y,C); blue basic residues (R,K,H); yellow hydrophilic residues (Q,N,S); gray, borderline residues (G,T,P).

coworkers utilized an *in silico* approach to identify a cluster of nine residues, from Leu-141 to Leu-149 that, when chemically synthesized in the form of a tandem repeat peptide called ApoEdp (Fig. 1C), showed significant antimicrobial activity that was absent in the nine-residue peptide alone [26].

More recently, a new ApoE peptide (named ApoE23) was designed, by combining synthetic fragments 141–148 and 135–149 (Fig. 1C). Like ApoEdp, ApoE23 contains a repeated module but in this case, a five-residue RLASH sequence was inserted between the two repeats. ApoE23 elicited a slightly stronger antimicrobial activity than ApoEdp and showed immunomodulatory effects on THP-1 cells [27].

Recently, our group has developed a bioinformatic method (K. Pane , L. Durante, O. Crescenzi, V. Cafaro, E. Pizzo, M. Varcamonti, A. Zanfardino, V. Izzo, A. Di Donato & E. Notomista, unpublished data) that identifies AMPs within the sequences of larger protein precursors and quantitatively predicts their antibacterial activity. The method assigns an antimicrobial score to peptides based on their net charge, hydrophobicity, and length, and two bacterial strain-dependent weight factors. We have demonstrated that the antimicrobial score is proportional to the antimicrobial activity of AMPs, at least for score values in the range of 6.5–9.5. Scores lower than 6.5 can be considered not significant as they correspond to predicted MIC values higher than 200 μM. However, for score values higher than 10, the linear relationship is no longer valid (i.e. for score values higher than 10, an increase in the score does not necessarily correspond to an increase in the antimicrobial activity). The score values of all the peptides of the desired lengths inside a protein can be plotted as a function of their length and position, thus creating an accurate map of the antimicrobial activity determinants. Figure 2 shows the isometric plot for the region 123–168 of ApoE. The known antimicrobial peptide 133–162 corresponds exactly to a relative maximum (score = 11.8) in the isometric plot. The absolute maximum, corresponding to region 133–167, is only slightly higher (score = 12.3). Very interestingly, the plot shows a relative maximum corresponding to residues 133–150 with score (score = 11.8) similar to that of peptide 133–162. Peptide ApoE (133–150) is only one residue longer than the synthetic peptide COG-133 (residues 133–149). It is worth noting that while COG-133 has been thoroughly studied for its anti-inflammatory and neuroprotective activities, to the best of our knowledge, its antimicrobial properties have never been investigated. However, peptides ApoEdp and ApoE23 possess high antimicrobial activity but they are artificial peptides including two copies of receptor-binding region (residues 141–149). Figure 1C compares sequences, chain termini groups, and calculated antimicrobial scores of peptides ApoEdp, ApoE23, COG-133, and ApoE (133–150).

Based on these considerations, we hypothesized that ApoE (133–150) could possess antimicrobial activity comparable to that observed for ApoEdp and ApoE23 while retaining the pharmacological properties of COG-133. Accordingly, the aim of this study was to analyze the structure, antimicrobial activity, cytotoxic effects on eukaryotic cells, and anti-inflammatory properties of peptide ApoE (133–150). Using a recently developed method for high-yield production of antimicrobial peptides in *E. coli* [34], we produced recombinant peptide ApoE (133–150), herein named $rApoE_{PM}$ (133–150), as it contains two additional residues (PM) at the N terminus, and compared its biological activities to those of three peptides obtained by chemical synthesis: sApoE (133–150), Ac-ApoE (133–150)-NH_2, and COG-133 [Ac-ApoE (133–149)-NH_2]. The biological activities of ApoE-derived peptides were also compared to those of peptide GKY20, a previously studied 20-residue 'cryptic' antimicrobial peptide, from the C-terminal region of human thrombin heavy chain [6] (Fig. 1C).

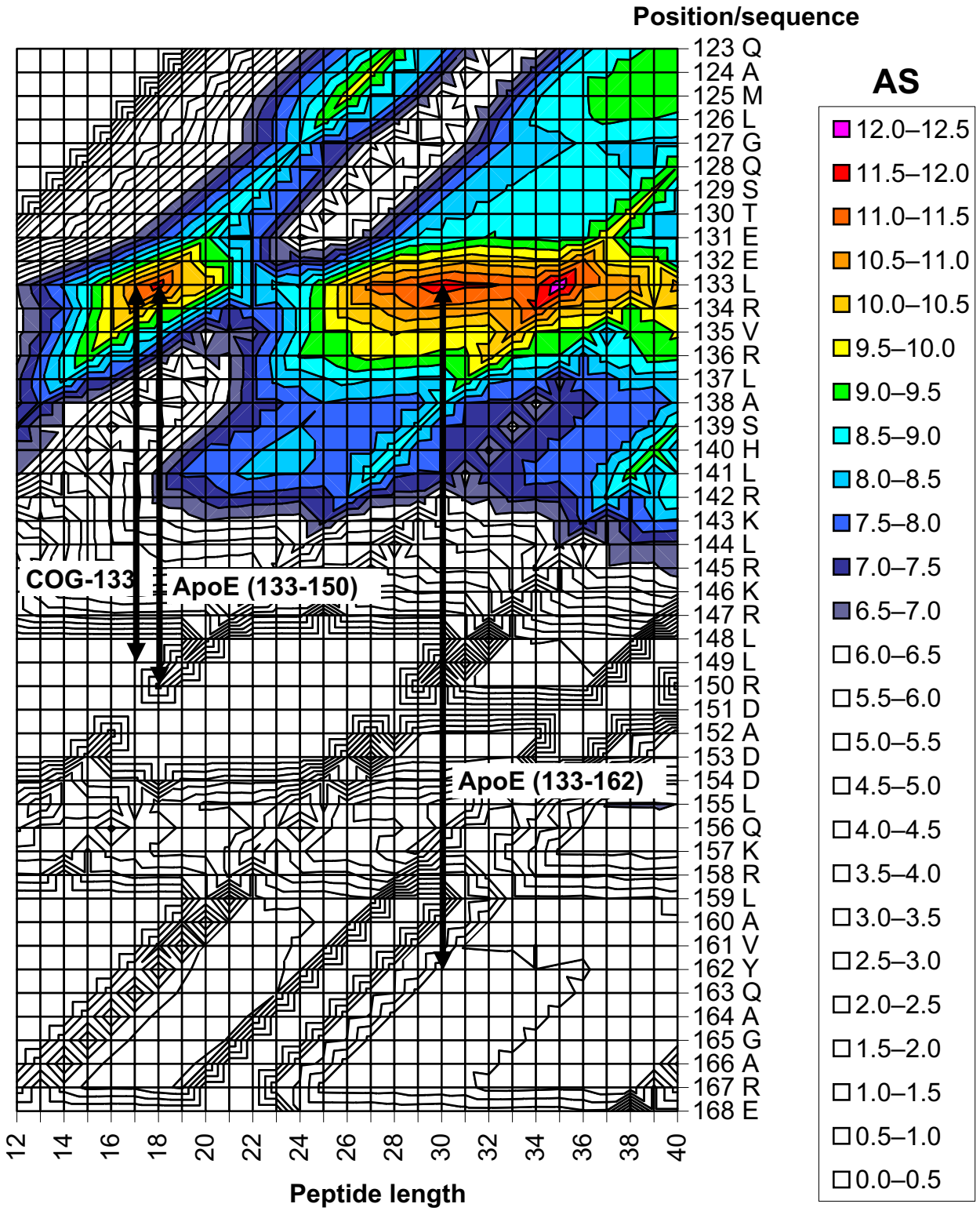

Fig. 2. Isometric plot showing the antimicrobial score (AS) values of peptides from 12 to 40 residues in the region 123–168 of ApoE obtained using parameters optimized for strain *S. aureus* C623. Colors were used to highlight antimicrobial score values higher than 6.5 corresponding to theoretical MIC values lower than 200 μM.

Results

Recombinant production of ApoE (133–150) and of control peptide GKY20

Expression of AMPs in bacterial cells can be deleterious to the host due to their toxicity. For this reason, we have developed a procedure to produce AMPs as fusion proteins with onconase (ONC), a frog ribonuclease that very efficiently mediates delivery to inclusion bodies, thus avoiding toxicity problems. The optimization procedure and the features of the final optimized carrier, named ONC-DCless-H6, have been described in detail elsewhere [34]. Here, we will describe the preparation of the construct used for the preparation of the recombinant ApoE peptide. Briefly, coding sequence for ApoE (133–150) was synthesized (MWG Biotech) using the *E. coli* codon usage and cloned into the expression vector pET22b$^{(+)}$, fused downstream to ONC-DCless-H6. The resulting fusion protein, ONC-DCless-H6-(PM)ApoE, contains a His tag sequence between the ONC moiety and the ApoE moiety suitable for an easy purification of the fusion protein, a flexible linker (Gly-Thr-Gly), and a tripeptide (Asp-Pro-Met) allowing to separate the carrier from the peptide either by mild acidic cleavage (that cleaves the Asp-Pro bond) or by cyanide bromide cleavage (that cleaves the bond following the Met residues).

After expression of pET22b$^{(+)}$ construct in *E. coli* cells, strain BL21(DE3), inclusion bodies were collected and purified by affinity chromatography on Ni Sepharose™ 6 Fast Flow (GE Healthcare). Chromatographic fractions were pooled after 15% SDS/PAGE analysis, and extensively dialyzed against 0.1 M acetic acid pH 3 at 4 °C. Any insoluble material was removed by centrifugation and filtration. The solution containing the fusion construct was then acidified to pH 2 using 0.5M HCl to cleave the Asp-Pro-Met linker peptide, purged with N_2, and incubated at 60 °C for 24 h in a water bath. Following cleavage, the pH was increased to 7–7.2 with the addition of 1 M NH_3, and incubated overnight at 28 °C to selectively precipitate the carrier ONC-DCless-H6 that is insoluble at neutral or alkaline pH. The released peptide was isolated from the insoluble components through repeated cycles of centrifugation and finally lyophilized. The purity of the peptide was checked by SDS/PAGE and by mass spectrometry (performed by Dr. Antimo Di Maro, Second University of Naples). The peptide derived from the expression of Apo E (133–150) coding sequence yielded a molecular weight of 2513.46 Da, which was the expected molecular weight of peptide ApoE (133–150) with the addition of the dipeptide Pro-Met released by the acidic cleavage of the linker peptide Asp-Pro-Met. This peptide was named rApoE $_{PM}$ (133–150).

The peptide GKY20, used as positive control in this study, corresponds to residues 231–250 of human thrombin heavy chain. Recombinant GKY20 was prepared as described for Apo E-derived peptide with the exception that in the fusion protein, the sequence of the peptide is preceded by the sequence Asp-Pro. Therefore, this peptide can be released only by acidic cleavage and contains an additional proline residue at the N terminus. Mass analysis of the recombinant peptide, herein named r(P)GKY20, yielded the expected molecular weight of 2609 Da. The full description of the preparation of r(P) GKY20 is reported elsewhere [34].

Antimicrobial activity of ApoE (133–150)

The antibacterial activity of synthetic and recombinant peptides was determined by measuring their MIC values on a panel of Gram-negative and Gram-positive strains (Table 1). In the case of Gram-negative strains, all the ApoE-derived peptides showed identical MIC values. Surprisingly, in the case of the two Gram-

Table 1. Antibacterial activity of Apo E-derived peptides.

	MIC (μM)[a]				
Bacterial strain	rApoE $_{PM}$ (133–150)	sApoE (133–150)	Ac-ApoE (133–150)-NH_2	Cog-133	r(P)GKY20
Escherichia coli DH5α	12.5	12.5	12.5	12.5	12.5
E. coli ATCC 25922	6.25	6.25	6.25	6.25	25
P. aeruginosa PAO1	25	25	25	25	25
P. aeruginosa PA14	50	50	50	50	50
K. pneumoniae ATCC 700603	6.25	6.25	3.12	3.12	12.5
S. aureus ATCC 6538P	3.12	3.12	100	100	6.25
B. subtilis PY79	25	25	> 100	> 100	12.5

[a]MIC values shown in the table are the highest concentrations obtained after three independent experiments.

positive strains, the synthetic peptides with modified chain termini, COG-133 and Ac-ApoE (133–150)-NH_2, showed very high MIC values. However, MIC values of unmodified rApoE $_{PM}$ (133–150) and sApoE (133–150) were identical and similar to those measured in the case of Gram-negative strains. Peptide GKY20 showed MIC values similar or slightly higher than those of rApoE $_{PM}$ (133–150) and sApoE (133–150) on all the strains with the exception of strain *B. subtilis* PY79. Therefore, it can be concluded that peptide ApoE (133–150) has antimicrobial activity similar to that of the thrombin-derived antimicrobial peptide and that this activity is strongly affected by modification of the chain termini.

When the killing rate of rApoE $_{PM}$ (133–150) and of r(P)GKY20 was assessed in buffer (Fig. 3A,B), rApoE $_{PM}$ (133–150) displayed antibacterial killing activity against *S. aureus* ATCC 6538P and a clinical isolate of *P. aeruginosa* strain KK27, substantially higher than that measured for r(P)GKY20. The antibacterial killing activity of rApoE $_{PM}$ (133–150) was also demonstrated for other bacterial strains showing in all cases a dose–response antibacterial activity (data not shown).

Recombinant rApoE $_{PM}$ (133–150) contains two additional amino acids, a Pro and a Met residue at the N terminus, compared to ApoE (133–150). To verify that the bactericidal action of rApoE $_{PM}$ (133–150) was not influenced by the presence of these additional residues, we compared the antibacterial activity of chemically synthesized ApoE (133–150) [sApo E (133–150)] with that of rApoE $_{PM}$ (133–150) on *E. coli* DH5α cells (Fig. 3C). We found that the bactericidal activity of both peptides was dose-dependent and quite similar (Fig. 3C). This indicated that the presence of the additional residues in rApoE$_{PM}$ (133–150) did not influence the antimicrobial activity of this peptide.

Conformational studies of rApoE $_{PM}$ (133–150) by circular dichroism

Far-UV CD spectra indicated that rApoE $_{PM}$ (133–150) was largely unstructured in PBS but became increasingly structured in the presence of TFE and SDS micelles (Fig. 4A–B) thus suggesting that rApoE $_{PM}$ (133–150), like other AMPs [35,36], is prone to assume a specific conformation when interacting with membrane-mimicking agents. At high concentrations of TFE and SDS, the CD spectra showed two broad minima, at 208 and 222 nm respectively, and one maximum at < 200 nm, indicative of the presence of α-helical conformation. A similar behavior could be observed also for control peptide r(P)GKY20 (Fig. 4C–D). It is worth noting that maximal

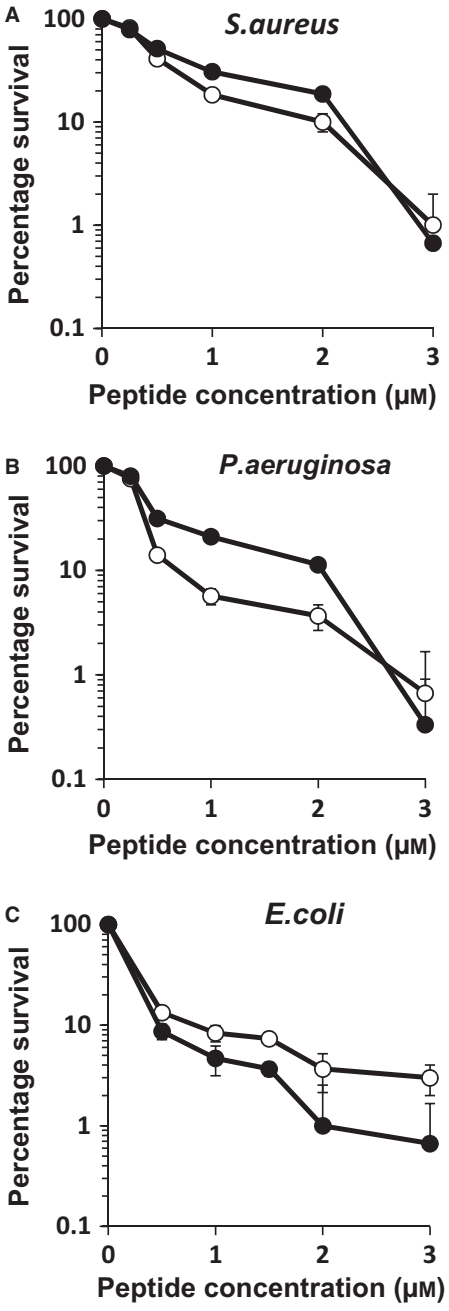

Fig. 3. Antibacterial activity of recombinant ApoE $_{PM}$(133–150) (white circles) compared to that of r(P)GKY20 (black circles). (A) *Staphylococcus aureus* ATCC 6538P. (B) *Pseudomonas aeruginosa* KK27. (C) Antibacterial activity of recombinant ApoE $_{PM}$(133–150) (white circles) compared to that of synthetic ApoE (133–150) (black circles). The mean values ± SD from three independent experiments run in triplicate are shown.

structured conformation was observed at a TFE concentration of about 40%, (Fig. 5), thus indicating a high propensity for rApoE $_{PM}$ (133–150) to acquire an ordered structure.

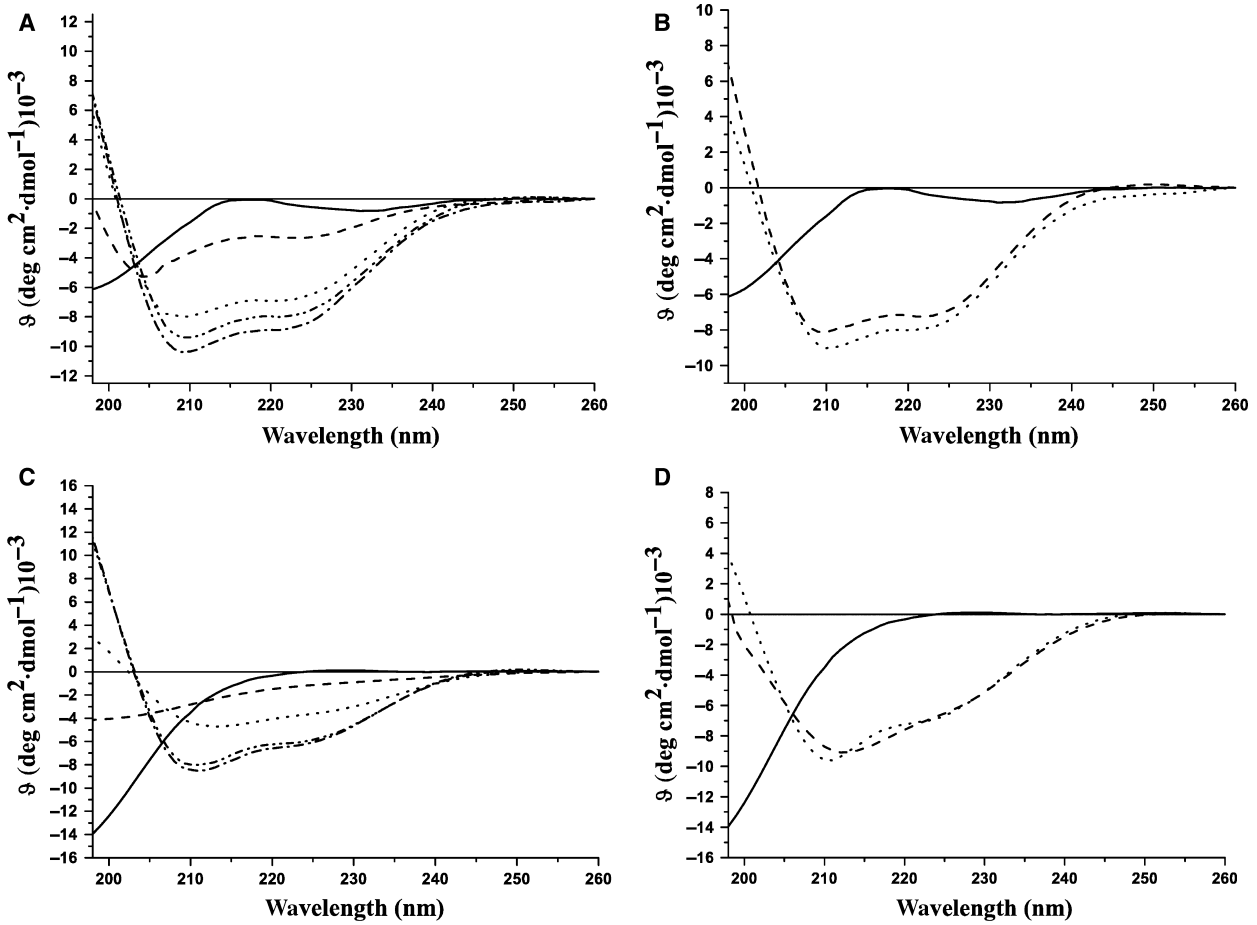

Fig. 4. CD spectra of the recombinant peptides in the presence of membrane-mimicking agents (TFE or SDS). rApoEPM(133–150) spectra in the presence of different concentrations of TFE (A) or SDS (B). r(P)GKY-20 spectra in the presence of different concentrations of TFE (C) or SDS (D). Panels (A) and (C): peptide in PBS (continuous line) or 10% TFE (—); 20% (••••); 40% (-••-); 50% (-•-•-). Panels (B) and (D): peptide in PBS (continuous line) or 10 mM SDS (—); 20 mM SDS (••••).

To further characterize the structural properties of rApoE $_{PM}$ (133–150), we analyzed by CD spectroscopy its binding to LPS (Fig. 6A), the main constituent of the outer membrane of Gram-negative bacteria. When rApoE $_{PM}$ (133–150) was analyzed in the presence of increasing concentrations (0.2 to 1.6 mg·mL^{-1}) of LPS purified from *P. aeruginosa* (Fig. 6A) or LPS purified from *E. coli* strain 0111:B4 (data not shown), two minima around 208 and 222 nm appeared, suggesting that the peptide adopts a helical conformation also upon interaction with LPS. Similar results were obtained also for r(P)GKY-20 in the presence of LPS as showed in Fig. 6B.

It is well known that alginate, an exopolysaccharide abundant in the biofilm of several bacterial strains, interacts with some AMPs and induces α-helical structure [37]. Therefore, we titrated our peptides with increasing concentrations of alginate (from 0.2 to 1.6 mg·mL^{-1}). The spectra recorded in the presence of alginate for both peptides (Fig. 6C,D) displayed shapes very different from those observed in TFE, SDS, and LPS. The saturation curves in Fig. 5D clearly show the interaction of r(P)GKY-20 with alginate. The spectra at the highest alginate concentrations are characterized by a single minimum between 215 and 220 nm, thus suggesting an extended conformation. However, spectra obtained in the case of rApoE $_{PM}$ (133–150) are rather complex and difficult to interpret; therefore, at the moment it is not clear if rApoE $_{PM}$ (133–150) does interact with alginate or what type of structure it adopts.

Cytotoxicity assays of rApoE $_{PM}$ (133–150) on human cells

As already mentioned, the promising interest in the use of AMPs as alternative antibiotics stems from their selective action on bacterial cells compared to

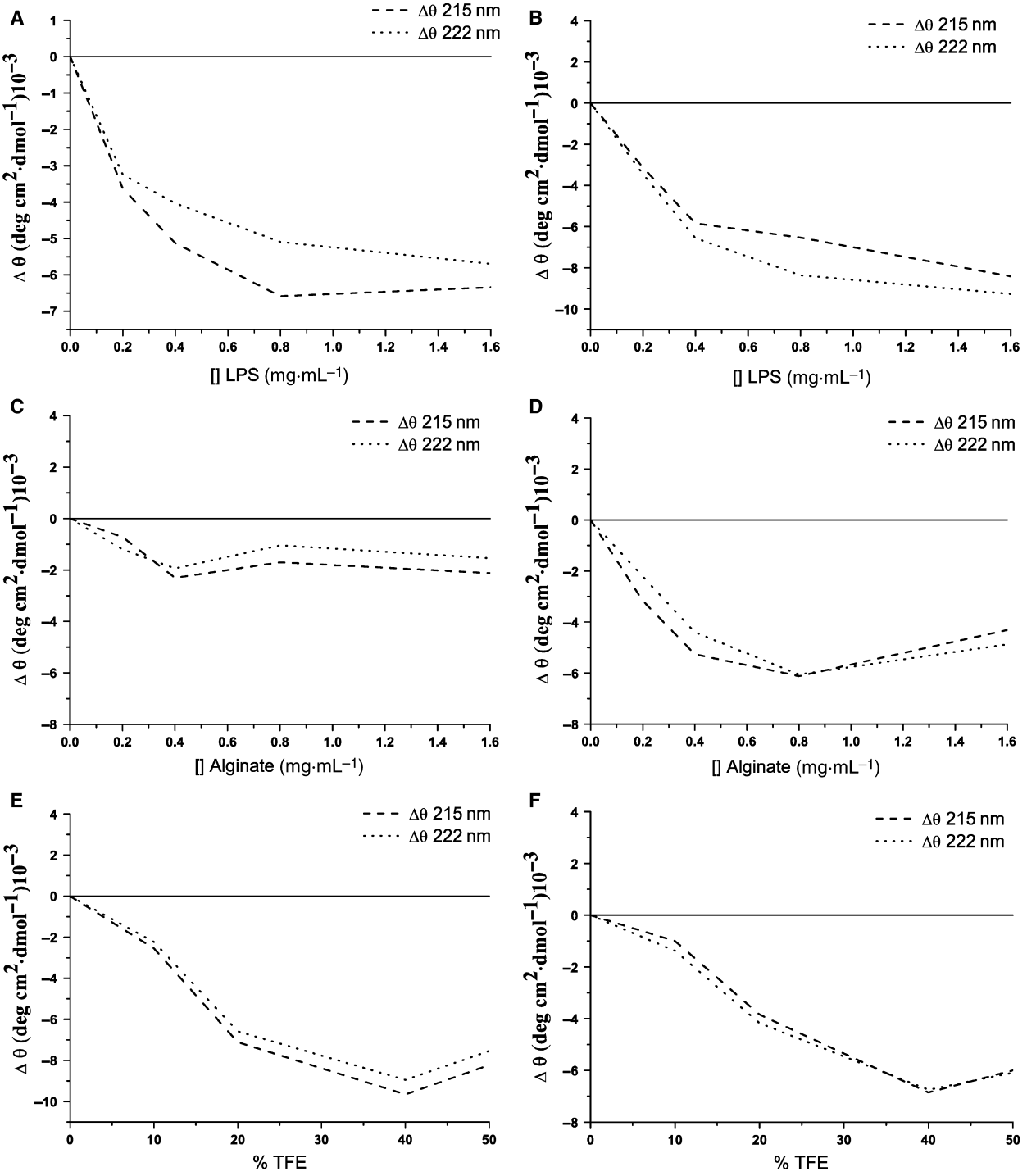

Fig. 5. Δθ at different wavelength of the recombinant peptides in the presence of different additive. Δθ were obtained by subtracting θ of peptides in the presence of different concentrations of additive at θ of peptides in PBS, pH 7.4. Δθ of $rApoE_{PM}$ (133–150) in the presence of different concentrations of LPS from *P. aeruginosa* (A), alginate (C), or TFE (E). Δθ of r(P)GKY20 in the presence of different concentrations of LPS from *P. aeruginosa* (B), alginate (D), or TFE (F).

eukaryotic cells. We thus studied the cytotoxic effect of $rApoE_{PM}$ (133–150) and of its synthetic form on either suspension or adherent human cell lines. The addition of increasing concentrations (1, 5, and 10 μM) of $rApoE_{PM}$ (133–150) or sApoE (133–150) to THP-1 cells, at three different incubation times,

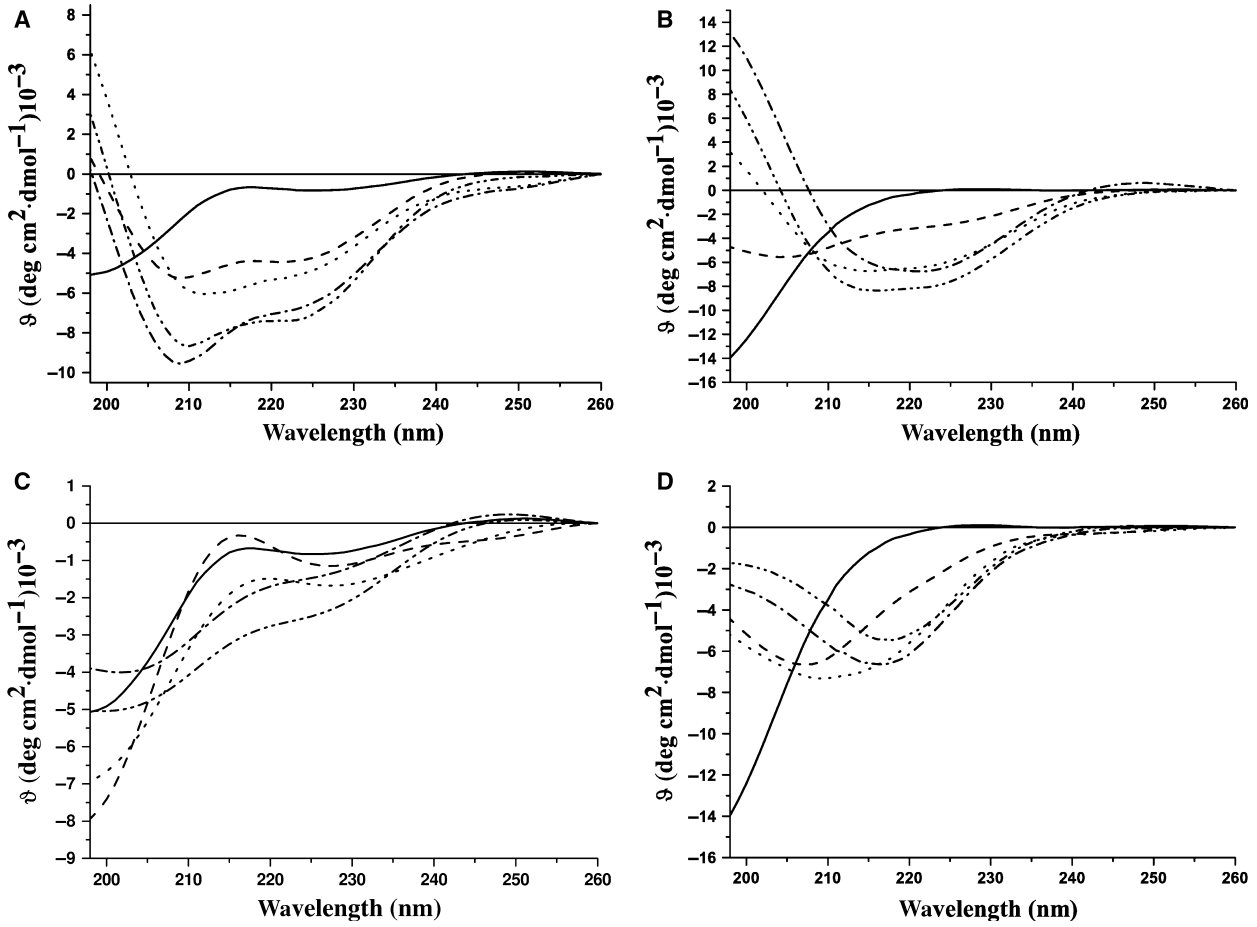

Fig. 6. CD spectra of the recombinant peptides in the presence of different concentrations of LPS. rApoE$_{PM}$(133–150) in the presence of different concentrations of LPS from *P. aeruginosa* (A) or alginate (C). r(P)GKY20 in the presence of different concentrations of LPS from *P. aeruginosa* (B) or alginate (D). Peptide alone (continuous line); 0.2 mg·mL^{-1} LPS (--); 0.4 mg·mL^{-1} LPS (····); 0.8 mg·mL^{-1} LPS (-·-·-); 1.6 mg·mL^{-1} LPS (-··-).

did not result in any significant reduction in cell viability (Fig. 7). Both peptides exhibited the same behavior, further supporting the conclusion that the two additional residues in the recombinant peptide (Pro-Met) do not influence its biological activity. The cytotoxicity of rApoE $_{PM}$ (133–150) was also measured against PMA-differentiated THP-1 cells, human keratinocytes (HaCat cells), and on three human tumor cells line (HeLa, HEK, and CaCo-2 cells). In all cases, no significant cytotoxicity was observed (data not shown), demonstrating that residues 133–150 ApoE do not exert any toxic effect on cultured human cells. Moreover, it should be mentioned that rApoE $_{PM}$ (133–150) and synthetic ApoE (133–150) are toxic to bacterial cells (Table 1) at concentrations similar to that used in the cytotoxicity assays described above.

Quantification of cytokine expression induced by rApoE $_{PM}$ (133–150)

It is known that several AMPs have the ability to block the production of cytokines produced in response to LPS by either directly up-regulating inhibitory pathways in cells [38], or interfering with the ability of LPS to bind LPS-binding proteins [39]. In order to investigate the hypothesis that rApoE $_{PM}$ (133–150) might elicit anti-inflammatory effects, and thus immunomodulatory activities on human cells, we analyzed the effects of rApoE $_{PM}$ (133–150), compared to sApoE (133–150), Ac-ApoE (133–150)-NH_2, and COG-133 on the LPS-induced Il-8 and Cox2 expression by qRT-PCR, in PMA-differentiated THP-1 cells. As shown in Fig. 4, in macrophages stimulated with LPS (THP-1D) in the presence of rApoE $_{PM}$ (133–150), we observed a

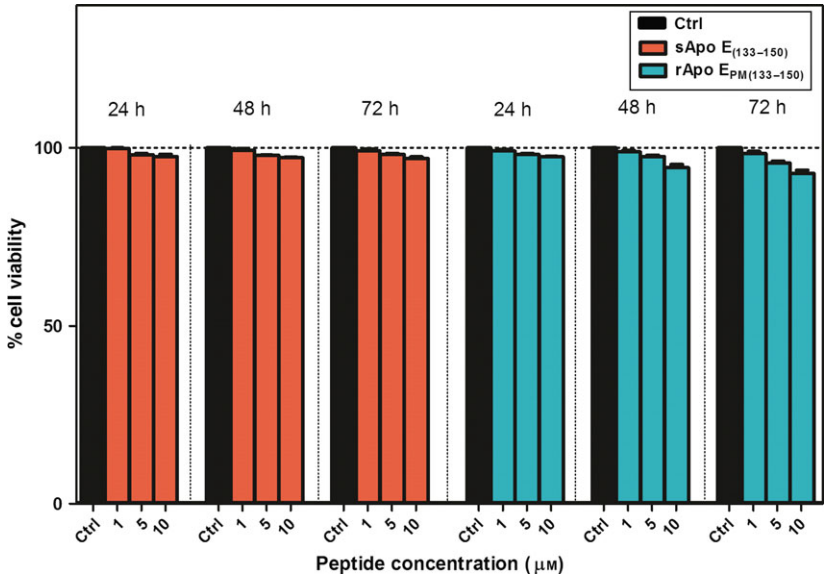

Fig. 7. Effect of synthetic ApoE (133–150) or rApoE $_{PM}$(133–150) on the viability of THP-1 cells. The mean values ± SD from three independent experiments run in triplicate are shown.

decrease in mRNA expression of IL-8 and Cox-2 (slightly more accentuated for IL-8), in comparison with macrophages treated with LPS alone (Fig. 4A). A similar effect, slightly less accentuated, was observed when differentiated THP-1 cells were treated with LPS in the presence of sApoE (133–150), COG-133, and Ac-ApoE (133–150)-NH_2. Interestingly, when undifferentiated THP-1 cells (THP-1U) were treated with LPS in the presence of rApoE $_{PM}$ (133–150), as well as for the other peptides, no relevant effects were observed on cytokines expression (Fig. 8A–B).

Although rApoE $_{PM}$ (133–150) does not seem to have a large effect on Cox-2 and IL-8 expression in undifferentiated THP-1 cells, we found that it was able to induce an immune response. Literature data demonstrated that LPS stimulation of THP-1 cells, normally nonadherent in culture, increases cell adhesion in a dose-dependent manner inducing cytoskeletal reorganization and increasing spreading in adherent THP-1 cells [40]. On this basis, we investigated the peptide effect on LPS action on cell adhesion in THP-1 cells.

In particular, the effects of rApoE $_{PM}$ (133–150) on LPS-induced adhesion of THP-1 cells were determined after 3 h of treatment by RTCA. Results indicated that the addition of 3 μM rApoE PM (133–150) induces an alteration in the adhesion curve relative to LPS-stimulated THP-1 in the absence of peptide (control), thus indicating a reduction of the capability of LPS-treated THP-1 to adhere to the plate surface (Fig. 8C).

The same effect of adhesion capabilities for THP-1 was observed on plates coated with fibronectin after 7 h (data not shown).

To further investigate the immunomodulatory properties of ApoE (133–150), peripheral blood mononuclear cells (PBMCs) isolated from donors were stimulated with LPS in the presence of increasing doses of sApoE (133–150), and the amount of TNF-α released was measured by ELISA. A synthetic innate defense regulator peptide, IDR-1018, which has previously been shown to possess immunomodulatory properties [41], was included as a positive control. As shown in Fig. 9A, LPS-stimulated PBMCs treated with sApoE (133–150) caused a significant reduction in the amount of TNF-α released, similar to the suppression observed in IDR-1018-treated cells. In terms of concentration, TNF-α released from PBMCs stimulated with LPS alone was of 1478.38 $pg{\cdot}mL^{-1}$, whereas TNF-α released from PBMCs stimulated with LPS and treated with sApoE (133–150) or IDR-1018 were of 683.63 and 479.17 $pg{\cdot}mL^{-1}$, respectively.

We further investigated the ability of sApoE (133–150) to act on the host immune response by measuring its ability to induce the release of MCP-1 (monocyte chemotactic protein-1), a member of chemotactic cytokines mainly involved in leukocyte migration [42] to the site of infection. As shown in Fig. 9B, the addition of increasing amounts of sApoE (133–150) to PBMCs caused a dose-dependent release of MCP-1, comparable to that obtained using similar amounts of IDR-1018. On the basis of this result, it is intriguing to hypothesize that ApoE (133–150) could play a role in promoting migration and recruitment of monocytes/macrophages in response to inflammation and tissue injury.

Finally, as ApoE is known to be produced by skin cells [43], and as the pathogenesis of many

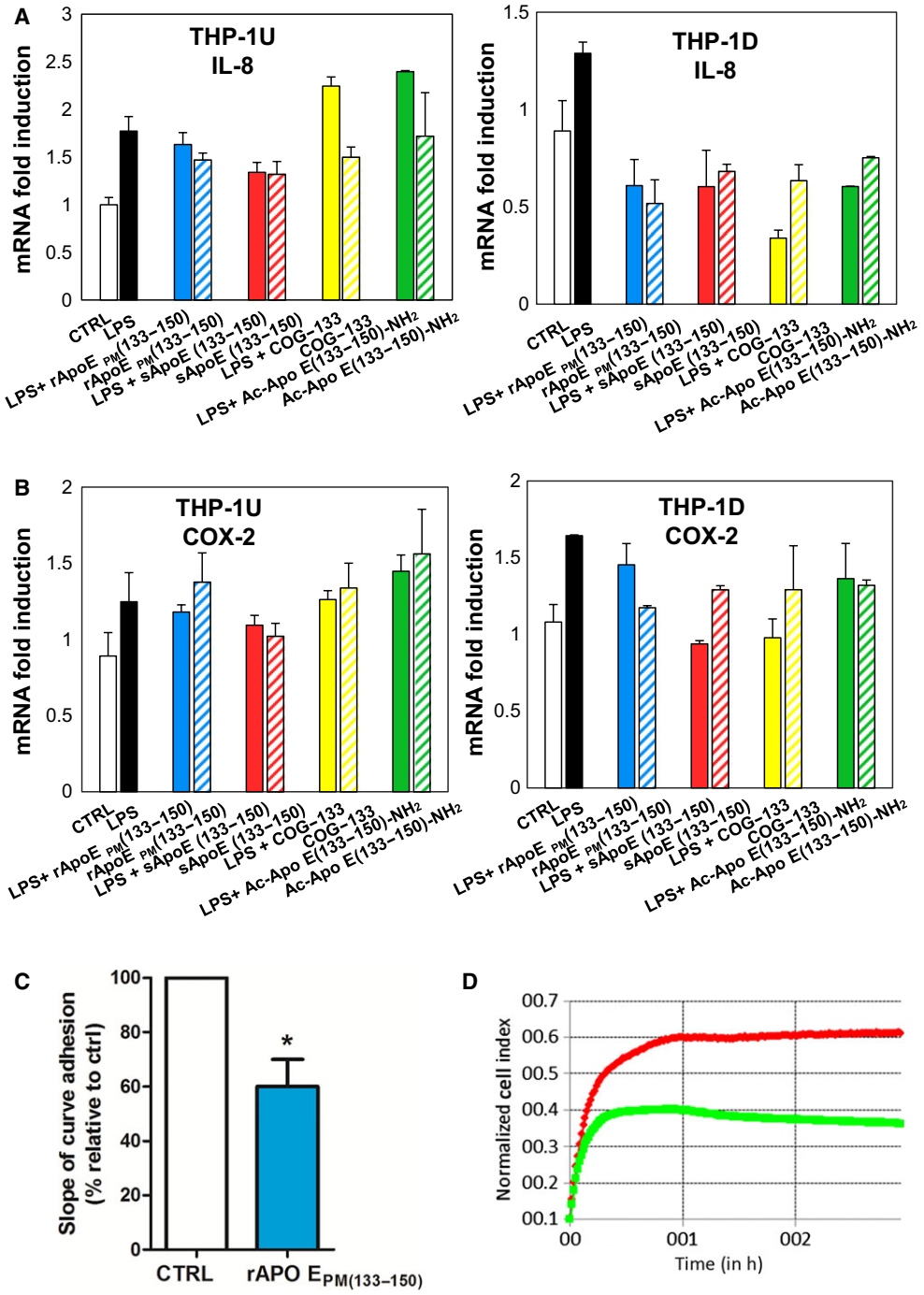

Fig. 8. Influence of ApoE-derived peptides in THP-1 cells treated with LPS, on gene expression of COX-2 (Panel A) and IL-8 (Panel B), and effect of rApoE $_{PM}$(133–150) on cellular adhesion (Panel C). Panels A and B: total RNA was isolated by two different cell lines THP-1D (Differentiated) and THP-1U (Undifferentiated): untreated (white bars), LPS-treated only (black bars), after exposition to LPS and ApoE-derived peptides (colored bars), and after exposition to peptides alone (diagonally colored bars). The results were expressed as relative fold induction respect to actin gene expression for A) COX-2 and B) IL-8. Data points represent the average of three independent experiments ± SE. Panel C: Slope of curve adhesion. LPS-treated THP-1 cells were incubated with 3 μM rApoE $_{PM}$(133–150) in a range of 0–3 h. Results are presented as the percentage of slope of adherent cells versus control (LPS-stimulated THP-1 in the absence of peptide) and are expressed as mean ± SE from three independent experiments performed in duplicate. Statistical significance based on Student's *t*-test (*$P < 0.05$). In Panel D, representative adhesion curves are reported: LPS-stimulated THP-1 in the absence (red) or presence (green line) of peptide.

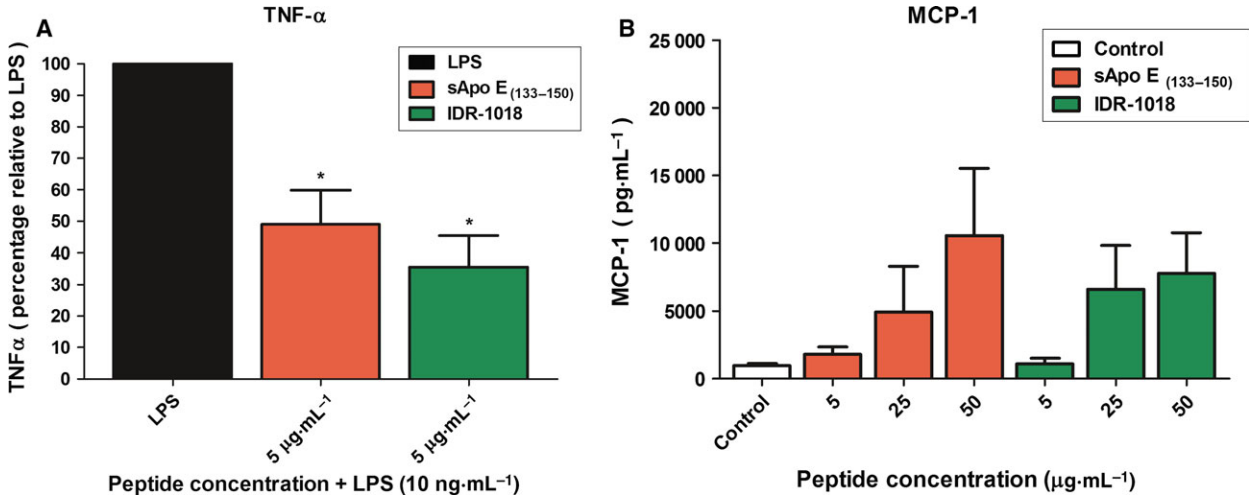

Fig. 9. Immunological response of human peripheral blood mononuclear cells (PBMCs) mediated by rApoE $_{PM}$(133–150). Panel A. Reduction of LPS-induced TNF-α cytokine. PBMCs stimulated with 10 ng·mL^{-1} of *P. aeruginosa* LPS were treated with rApo E $_{PM}$(133–150) or with the strongly immunomodulatory peptide IDR-1018. TNF-α secretion was measured by ELISA after 24 h of incubation. Peptide activities are reported as percentage of TNF-α released compared with LPS alone. Panel B. Induction of MCP-1 chemokine. PBMCs were treated with rApo E $_{PM}$(133–150) or with the strongly immunomodulatory peptide IDR-1018, at three different concentrations. MCP-1 secretion was measured by ELISA after 24 h of incubation. Peptides activities are reported as amount of MCP-1 released compared with untreated cells (control). The results represent mean ± SEM of two replicates of five independent donors. The results represent mean ± SEM of two replicates of three independent donors. Statistical significance based on Student's *t*-test (*$P < 0.05$ compared with LPS).

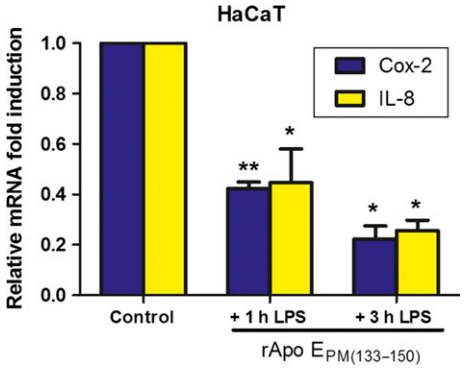

Fig. 10. Influence of rApoE $_{PM}$(133–150) on COX-2 and IL-8 gene expressions, in HaCaT cell lines, pretreated with LPS. Total RNA was isolated by human keratinocytes, HaCaT cell lines, pretreated with LPS, and exposed to ApoE for 1 h or 3 h. The results were expressed as relative fold induction respect to 18S. Data points represent the average of three independent experiments ± SE. Statistical significance based on Student's *t*-test (*$P < 0.05$; **$P < 0.01$ compared to respective untreated control cells).

inflammatory skin diseases is due to an immune response involving keratinocytes, immune cells, and soluble mediators [44], we investigated the possibility that rApoE $_{PM}$ (133–150) could have immunomodulatory properties on keratinocytes. The anti-inflammatory effect of rApoE $_{PM}$ (133–150) on the expression of proinflammatory cytokines COX-2 and IL-8 was measured in LPS pretreated HaCaT cells. The results shown in Fig. 10 clearly demonstrate that rApoE$_{PM}$ (133–150) was able to dramatically down-regulate the expression of both COX-2- and IL-8-encoding genes. Similar results have been obtained also for sApoE (133–150) (data not shown).

Discussion

Cationic antimicrobial peptides (AMPs) are ancestral elements of the innate immune system and are virtually present in all multicellular organisms. The majority of AMPs share common biochemical features, including relatively small size, cationicity, and amphipathicity. These features are believed to be essential for the antimicrobial activity of AMPs, allowing them to selectively interact with and damage bacterial membranes. Interestingly, a wide variety of human proteins whose primary functions are not necessarily related to host defense, contain AMPs hidden inside their sequence [45–47]. These 'cryptic' AMPs have attracted the interest of researchers for many different reasons. The existence of cryptic AMPs would suggest that innate immunity is more complex and includes more components than usually believed. The immunomodulatory effects of these AMPs further support the idea that adaptive and innate immunity are tightly coregulated. Finally, it is tempting to speculate that human proteome is a yet unexplored source of bioactive

peptides with many potential pharmacological applications.

Apolipoprotein E (ApoE) is a good example of protein that carries a cryptic AMP sequence. For a long time, ApoE was considered to simply be an important carrier of lipids in general and of cholesterol in particular. However, several recent studies have highlighted that it is endowed with anti-inflammatory, antiviral, and antimicrobial activities [48–50]. Even more intriguing is that peptides derived from the receptor-binding region of ApoE retain some of the most interesting pharmacological activities of the intact protein. For example, Ac-ApoE (133–149)-NH_2, the so-called COG-133 peptide, and ApoE (133–162) show anti-inflammatory/neuroprotective activity and antimicrobial activity, respectively [51,52]. Other groups have also designed artificial peptides with duplicated regions derived from ApoE fragments that show both antimicrobial and anti-inflammatory activity (e.g. peptides ApoEdp and ApoE23 described in the introduction). Recent reports [27–31] have shown that artificial peptides derived from ApoE receptor-binding region share a broad anti-infective activity along with the presence of the positively charged leucine-rich sequence -RKLRKRLL- from residue 141 to 149.

This work demonstrates for the first time that an unmodified fragment derived from ApoE receptor-binding region (from residue 133 to residue 150), possesses both antimicrobial and anti-inflammatory/immunomodulatory activities. The experiments described in this paper show that synthetic ApoE (133–150) and its recombinant counterpart $rApoE_{PM}$ (133–150), both with unmodified chain termini, exhibited antibacterial activities against both Gram-positive and negative strains, including a pathogenic strains of *P. aeruginosa*, while having negligible cytotoxic effects on an assortment of human cell lines. From a structural point of view, in agreement with the canonical properties of most AMPs, we verified by CD that ApoE (133–150) tends to assume a conformation in the presence of mimic membrane agents, whereas it is unstructured in aqueous buffer. It should also be noted that ApoE (133–150) becomes structured in the presence of LPS, in a dose-dependent manner, thus suggesting direct binding to LPS.

Furthermore, our results showed that ApoE (133–150), significantly down-regulated the expression of IL-8, TNF-α, and Cox-2 in LPS-induced THP-1 and PBMCs cells, and induced a dose-dependent release of a chemotactic cytokine, MCP-1 from PBMCs. Additionally, ApoE (133–150) induced immunomodulatory activity in human keratinocyte cell lines, opening a new scenario on future topical application of human AMPs.

In conclusion, our data on ApoE (133–150) add new details for the development of novel antibacterial drugs that target MDR strains among others. Compared to other antimicrobial agents, ApoE (133–150) may offer several advantages, as it specifically targets bacterial strains, reduces the likelihood of developing resistance and at the same time contributes to enhance anti-inflammatory response without altering cell viability. Thus, by virtue of its different mechanism of action, ApoE (133–150) could be used in combination with other antibiotic drugs to obtain potential synergistic effects in treating bacterial infections. Finally, we have shown that peptide ApoE (133–150) can be produced in a fully active recombinant form in high yields using the fusion system recently developed by our group. This will further promote the development of its potential applications.

Materials and methods

Peptide synthesis

ApoE (133–150) peptides were synthesized by Thermo Fisher Scientific GmbH (Ulm, Germany) or PEPTIDE 2.0 (Chantilly, VA, USA) using solid-phase 9-fluorenylmethoxy carbonyl (Fmoc) chemistry with a free C terminus and purified to a purity > 95% using reverse-phase high-performance liquid chromatography (HPLC). COG-133 and Ac-ApoE (133–150)-NH_2 were synthesized and purified to 95% homogeneity by Inbios (Naples, Italy). Peptide masses were confirmed by mass spectrometry.

Antimicrobial assays

The antimicrobial activity of peptides was measured against *Escherichia coli* DH5α, *Escherichia coli* ATCC 25922 provided by Dr. Eliana De Gregorio (University of Naples Federico II, Italy); *Staphylococcus aureus* ATCC 6538P; and *Pseudomonas aeruginosa* KK27, a clinical isolated strain obtained from cystic fibrosis patients and provided by Dr. Alessandra Bragonzi (San Raffaele Hospital, Milan, Italy).

MIC values were determined on strains *Escherichia coli* ATCC 25922 (provided by Dr. Eliana De Gregorio, University of Naples Federico II, Italy), *Pseudomonas aeruginosa* PAOI and PA14, *Klebsiella pneumoniae* ATCC 700603, and *Bacillus subtilis* PY79 using the broth microdilution method for cationic peptides [53] with minor modifications. The assay was performed in Difco Nutrient Broth (Becton-Dickenson, Franklin Lakes, NJ, USA) using a bacterial inoculum of $\sim 5 \times 10^5$ CFU·mL^{-1} per well.

Rate of killing was measured according to Pizzo *et al.* [54]. All compounds were tested in triplicate experiments. Standard deviations were always < 5% for each experiment.

MTT assays

Cytotoxicity on normal or tumoral cells (HaCat, undifferentiated THP-1, PMA-differentiated THP-1, HeLa, CaCo-2, and HEK) was assessed by performing the 3-(4,5-dimethylthiazol-2-yl)-2,5 diphenyltetrazolium bromide (MTT) reduction inhibition assay [55]. Cytotoxicity experiments were performed at least three times independently. Standard deviations were always < 5% for each experiment.

Circular dichroism spectroscopy

Circular dichroism (CD) spectra of $rApoE_{PM}$ (133–150) or r(P)GKY-20 (recombinant versions of peptides showed in Fig. 1C) were recorded with a J-810 spectropolarimeter equipped with a Peltier temperature control system (Model PTC- 423-S; Jasco Europe, Cremella, LC, Italy). Far-ultraviolet (far-UV) measurements (197–260 nm) were carried out at 20 °C using a 0.1 cm optical path length cell and a peptide concentration of 50 μM. CD spectra, recorded with a time constant of 4 s, a 2 nm bandwidth, and a scan rate of 10 $nm \cdot min^{-1}$ were signal-averaged over at least three scans. The baseline was corrected by subtracting the complete buffer spectrum. CD spectra in the presence of LPS from *Pseudomonas aeruginosa* strain 10 [(Sigma Aldrich, Milan, Italy) purified by phenol extraction] or alginate (Sigma Aldrich) were recorded using different concentrations of each compound (ranging from 0.2 to 1.6 $mg \cdot mL^{-1}$) and the baseline was corrected by subtracting the spectrum of LPS and alginate alone at the same concentration. Additional CD spectra were acquired in the presence of different concentrations of SDS or trifluoroethanol (TFE). Prediction analysis of secondary structure content was performed with CDPro.

Real-time quantitative PCR (qRT-PCR)

Either human immortalized keratinocytes (HaCaT) or undifferentiated monocyte/macrophage (THP-1) cells or PMA (2 nM)-differentiated THP-1 cells were cultured in six-well tissue culture plates (8×10^5 $cells \cdot well^{-1}$); cell culture dish with 2 mm grid pretreated for 3 h at 37 °C with 50 $ng \cdot mL^{-1}$ LPS from *P. aeruginosa* P10 strain. Cells were then treated with 3 μM $rApoE_{PM}$ (133–150), sApoE (133–150), COG-133, Ac-ApoE (133–150)-NH_2, or buffer, and incubated at 37 °C for 1 h or 3 h. Alternatively, a coincubation with 1 $\mu g \cdot mL^{-1}$ LPS and 3 μM $rApoE_{PM}$ (133–150) was performed for 6 h. Following incubation, cells were washed twice using ice-cold PBS pH 7.4. Total cellular RNA was isolated using TRI Reagent (Sigma Aldrich). Of total RNA, 1 mg was reverse transcribed using the QuantiTect RT-PCR Kit (Qiagen, Hilden, Germany) according to the manufacturer's instructions.

Real-time quantitative PCR (qRT-PCR) amplifications were performed using the *Power* SYBR® Green PCR Master Mix (Applied Biosystems, Foster City, CA, USA) in Applied Biosystems® 7500 Real-Time PCR Systems. The qRT-PCR conditions were: 95 °C for 15 min followed by 40 cycles of 95 °C for 15 s, 59 °C for 30 s, and 72 °C for 30 s. The following primers were used for cDNA amplification: COX-2 5′-TCACGCATCAGTTTTTCAAGA-3′ (*forward*) and 5′-TCACCGTAAATATGATTTAAGTCCAC-3′ (*reverse*); IL-8 5′-GGCACAAACTTTCAGAGACAG-3′ (*forward*) and 5′-ACACAGAGCTGCAGAAATCAGG-3′ (*reverse*); and as the housekeeping genes for the qRT -PCR reaction 18S rRNA (*forward*) 5′-TCGAGGCCCTGTAATTGGAA-3′ (*forward*) and 5′-CTTTAATATACGCTATTGGAGCTGG AA-3′(*reverse*); and actin: 5′-ATTGCCGACAGGATGCA-GAA-3′ (*forward*) and 5′-GCTGATCCACATCTGCTGG AA-3′ (*reverse*)). Results were expressed as relative fold induction of the target genes relative to the reference gene. Calculations of relative expression levels were performed using the $2^{-\Delta\Delta C}t$ method [56] and averaging the values of at least three independent experiments.

Cell isolation and peptide stimulation

Venous blood from healthy volunteers was collected in vacutainer collection tubes containing sodium heparin as anticoagulant (BD Biosciences, Franklin Lakes, NJ, USA), in accordance with University of British Columbia ethics approval and guidelines. All volunteers were informed of the experiments to be undertaken and written consent was obtained from each donor. Additionally, the methodologies used in these experiments conformed to the standards for nonclinical biomedical research set by the Declaration of Helsinki [57]. Blood was diluted with an equal volume of PBS (Invitrogen Life Technologies, Monza, Italy) and cells were separated by centrifugation using Lymphoprep (Stemcell Technologies, Vancouver, BC, Canada) as a density gradient medium. The buffy coat was collected and washed twice in PBS, and the number of PBMCs was determined by trypan blue exclusion. PBMCs were resuspended in RPMI 1640 medium, supplemented with 10% (v/v) heat-inactivated FBS, 2 mM L-glutamine, and 1 mM sodium pyruvate (all from Invitrogen Life Technologies). Cells were seeded into 96-well tissue culture plates at 1×10^6 $cells \cdot mL^{-1}$ at 37 °C in 5% CO_2, and rested for 1 h. Cells were then exposed to peptide at concentrations of 5, 25, and 50 $\mu g \cdot mL^{-1}$ for 24 h with or without 10 $ng \cdot mL^{-1}$ of LPS from *P. aeruginosa*. All experiments involved at least three biological replicates starting from three blood donors.

Detection of chemokines and cytokines

Following a 24-h exposure to the peptide, tissue culture supernatants were centrifuged at 145.8 ***g*** at 4 °C for 5 min in an IEC Micro-Max centrifuge to obtain cell-free samples. Supernatants were aliquoted and then stored at −20 °C before assaying for MCP-1 and TNF-α by sandwich ELISA (eBiosciences, Hatfield, UK). All assays were

performed in three separate experiments (from at least three blood donors). The concentration of chemokine/cytokine in culture medium was determined by establishing a standard curve with serial dilutions of recombinant human MCP-1 and TNF- α, respectively.

Adhesion analyses

The real-time cell analyzer (RTCA) and E-plate 16 system (xCELLigence; Roche, San Diego, CA, USA) allows monitoring of the viability of cultured cells using impedance by a label-free, real-time, noninvasive method [58]. This platform uses gold electrodes at the bottom of microplate wells as sensors to which an alternating current is applied. Cells are adherently grown in monolayers on top of the electrodes, affecting the alternating current at the electrodes by changing the electrical impedance, denoted as cell index (CI). Cell index values are proportional to the area of cells attached and to the total number of cells [59–61].

THP-1 adhesion induced by 1 $\mu g \cdot mL^{-1}$ LPS in the presence of $rApoE_{PM}$ (133–150) was monitored using the RTCA methodology. A total of 200 μL of cell culture media was added to E-plates (with or without fibronectin coating). After incubation at 23 °C for 15 min, the background intensity was measured. The adhesion capacity of THP-1 cells, which was visualized in increments of the CI, was determined according to the manufacturer's instructions. Briefly, 80 000 cells were suspended in 100 μL of serum-free medium and seeded into each well. Immediately, an E-plate was installed into the RTCA system, and the CI was measured every minute. The rate of cell adherence was determined by calculating the slope of the line between two given time points. The endpoint of the experiment corresponded to the maximum CI values observed for each adhesion curves.

Statistical analysis

Statistical significance between groups was assessed by Student's *t*-test. Data are expressed as means ± standard error (SE). All experiments were repeated at least three times. P values < 0.05 were considered to be statistically significant.

Acknowledgements

This research was supported by 'Italian Cystic Fibrosis Foundation'-grant FFC#20/2014 titled 'Identification and characterization of LPS-neutralizing human peptides: potential tools to control inflammation in cystic fibrosis lung disease'—principal investigator Elio Pizzo. Peptide research in the lab of REWH is supported by a grant from the Canadian Institutes of Health Research (CIHR) [funding reference number MOP-74493]. EFH was supported by a postdoctoral fellowship from the CIHR. REWH holds a Canada Research Chair. The authors are deeply indebted to Dr Valeria Pistorio for her experimental contributions and Dr Antimo Di Maro for mass spectra analysis and for his useful comments and suggestions.

Author contributions

KP, VS, prepared recombinants peptides and performed cytotoxicity experiments on eukaryotic cells, AZ performed antibacterial activity assays, GS and EmP performed circular dichroism experiments, EFH performed ELISA assays, TA, DC, and SDG performed qRT experiments and adhesion assay, VI, VC, MV, ADD, REWH analyzed data, EN and EP planned experiments and wrote manuscript.

References

1 Hilchie AL, Wuerth K & Hancock REW (2013) Immune modulation by multifaceted cationic host defence (antimicrobial) peptides. *Nat Chem Biol* **9**, 761–768.
2 Fjell CD, Hiss JA, Hancock REW & Schneider G (2012) Designing antimicrobial peptides: form follows function. *Nat Rev Drug Discov* **11**, 37–51.
3 Epand RM & Epand RF (2011) Bacterial membrane lipids in the action of antimicrobial agents. *J Pept Sci* **17**, 298–305. Review.
4 Wiesner J & Vilcinskas A (2010) Antimicrobial peptides: the ancient arm of the human immune system. *Virulence* **1**, 440–464. Review.
5 Hou S, Liu Z, Young AW, Mark SL, Kallenbach NR & Ren D (2010) Effects of Trp- and Arg-containing antimicrobial-peptide structure on inhibition of Escherichia coli planktonic growth and biofilm formation. *Appl Environ Microbiol* **76**, 1967–1974.
6 Kasetty G, Papareddy P, Kalle M, Rydengård V, Walse B, Svensson B, Mörgelin M, Malmsten M & Schmidtchen A (2011) The C-terminal sequence of several human serine proteases encodes host defense functions. *J Innate Immun* **3**, 471–482.
7 Lee DY, Huang CM, Nakatsuji T, Thiboutot D, Kang SA, Monestier M & Gallo RL (2009) Histone H4 is a major component of the antimicrobial action of human sebocytes. *J Invest Dermatol* **129**, 2489–2496.
8 Beck WH, Adams CP, Biglang-Awa IM, Patel AB, Vincent H, Haas-Stapleton EJ & Weers PM (2013) Apolipoprotein A-I binding to anionic vesicles and lipopolysaccharides: role for lysine residues in antimicrobial properties. *Biochim Biophys Acta* **1828**, 1503–1510.
9 Mahley RW (1988) Apolipoprotein E: cholesterol transport protein with expanding role in cell biology. *Science* **240**, 622–630.

10 Teoh CL, Griffin MD & Howlett GJ (2011) Apolipoproteins and amyloid fibril formation in atherosclerosis. *Protein Cell* **2**, 116–127.
11 Kim J, Basak JM & Holtzman DM (2009) The role of apolipoprotein E in Alzheimer's disease. *Neuron* **63**, 287–303.
12 Shi J, Zhao CB, Vollmer TL, Tyry TM & Kuniyoshi SM (2008) APOE epsilon 4 allele is associated with cognitive impairment in patients with multiple sclerosis. *Neurology* **70**, 185–190.
13 Coto-Segura P, Coto E, Alvarez V, Morales B, Soto-Sánchez J, Corao AI & Santos-Juanes J (2010) Apolipoprotein epsilon4 allele is associated with psoriasis severity. *Arch Dermatol Res* **302**, 145–149.
14 Baitsch D, Bock HH, Engel T, Telgmann R, Müller-Tidow C, Varga G, Bot M, Herz J, Robenek H, von Eckardstein A *et al.* (2011) Apolipoprotein E induces antiinflammatory phenotype in macrophages. *Arterioscler Thromb Vasc Biol* **31**, 1160–1168.
15 Curtiss LK, Forte TM & Davis PA (1984) Cord blood plasma lipoproteins inhibit mitogen-stimulated lymphocyte proliferation. *J Immunol* **133**, 1379–1384.
16 Tenger C & Zhou X (2003) Apolipoprotein E modulates immune activation by acting on the antigen-presenting cell. *Immunology* **109**, 392–397.
17 Riddell DR, Graham A & Owen JS (1997) Apolipoprotein E inhibits platelet aggregation through the L-arginine:nitric oxide pathway. Implications for vascular disease. *J Biol Chem* **272**, 89–95.
18 van den Elzen P, Garg S, León L, Brigl M, Leadbetter EA, Gumperz JE, Dascher CC, Cheng TY, Sacks FM, Illarionov PA *et al.* (2005) Apolipoprotein-mediated pathways of lipid antigen presentation. *Nature* **437**, 906–910.
19 de Bont N, Netea MG, Demacker PN, Verschueren I, Kullberg BJ, van Dijk KW, van der Meer JW & Stalenhoef AF (1999) Apolipoprotein E knock-out mice are highly susceptible to endotoxemia and *Klebsiella pneumoniae* infection. *J Lipid Res* **40**, 680–685.
20 Roselaar SE & Daugherty A (1998) Apolipoprotein E-deficient mice have impaired innate immune responses to Listeria monocytogenes in vivo. *J Lipid Res* **39**, 1740–1743.
21 Marques MA, Owens PA & Crutcher KA (2004) Progress toward identification of protease activity involved in proteolysis of apolipoprotein E in human brain. *J Mol Neurosci* **24**, 73–80.
22 Elliott DA, Tsoi K, Holinkova S, Chan SL, Kim WS, Halliday GM, Rye KA & Garner B (2011) Isoform-specific proteolysis of apolipoprotein-E in the brain. *Neurobiol Aging* **32**, 257–271.
23 Aono M, Bennett ER, Kim KS, Lynch JR, Myers J, Pearlstein RD, Warner DS & Laskowitz DT (2003) Protective effect of apolipoprotein E-mimetic peptides on N-methyl-D-aspartate excitotoxicity in primary rat neuronal-glial cell cultures. *Neuroscience* **116**, 437–445.
24 Croy JE, Brandon T & Komives EA (2004) Two apolipoprotein E mimetic peptides, ApoE(130-149) and ApoE(141-155)2, bind to LRP1. *Biochemistry* **43**, 7328–7335.
25 Clay MA, Anantharamaiah GM, Mistry MJ, Balasubramaniam A & Harmony JA (1995) Localization of a domain in apolipoprotein E with both cytostatic and cytotoxic activity. *Biochemistry* **34**, 11142–11151.
26 Forbes S, McBain AJ, Felton-Smith S, Jowitt TA, Birchenough HL & Dobson CB (2013) Comparative surface antimicrobial properties of synthetic biocides and novel human apolipoprotein E derived antimicrobial peptides. *Biomaterials* **34**, 5453–5464.
27 Wang CQ, Yang CS, Yang Y, Pan F, He LY & Wang AM (2013) An apolipoprotein E mimetic peptide with activities against multidrug-resistant bacteria and immunomodulatory effects. *J Pept Sci* **19**, 745–750.
28 Wilson C, Wardell MR, Weisgraber KH, Mahley RW & Agard DA (1991) Three-dimensional structure of the LDL receptor-binding domain of human apolipoprotein E. *Science* **252**, 1817–1822.
29 Raussens V, Slupsky CM, Ryan RO & Sykes BD (2002) NMR structure and dynamics of a receptor-active apolipoprotein E peptide. *J Biol Chem* **277**, 29172–29180.
30 Futamura M, Dhanasekaran P, Handa T, Phillips MC, Lund-Katz S & Saito H (2005) Two-step mechanism of binding of apolipoprotein E to heparin: implications for the kinetics of apolipoprotein E-heparan sulfate proteoglycan complex formation on cell surfaces. *J Biol Chem* **280**, 5414–5422.
31 Laskowitz DT, Thekdi AD, Thekdi SD, Han SK, Myers JK, Pizzo SV & Bennett ER (2001) Downregulation of microglial activation by apolipoprotein E and apoE-mimetic peptides. *Exp Neurol* **167**, 74–85.
32 Sarantseva S, Timoshenko S, Bolshakova O, Karaseva E, Rodin D, Schwarzman AL & Vitek MP (2009) Apolipoprotein E-mimetics inhibit neurodegeneration and restore cognitive functions in a transgenic *Drosophila* model of Alzheimer's disease. *PLoS One* **4**, e8191.
33 Azuma M, Kojimab T, Yokoyama I, Tajiri H, Yoshikawa K, Saga S & Del Carpio CA (2000) A synthetic peptide of human apoprotein E with antibacterial activity. *Peptides* **21**, 327–330.
34 Pane K, Durante L, Pizzo E, Varcamonti M, Zanfardino A, Sgambati V, Di Maro A, Carpentieri A, Izzo V, Di Donato A *et al.* (2016) Rational design of a carrier protein for the production of recombinant toxic peptides in *Escherichia coli*. *PLoS One* **11**, e0146552.
35 Subasinghage AP, O'Flynn D, Conlon JM & Hewage CM (2011) Conformational and membrane interaction studies of the antimicrobial peptide alyteserin-1c and its

analogue [E4K]alyteserin-1c. *Biochim Biophys Acta* **1808**, 1975–1984.
36 Gopal R, Park JS, Seo CH & Park Y (2012) Applications of circular dichroism for structural analysis of gelatin and antimicrobial peptides. *Int J Mol Sci* **13**, 3229–3244.
37 Chan C, Burrows LL & Deber CM (2004) Helix induction in antimicrobial peptides by alginate in biofilms. *J Biol Chem* **279**, 38749–38754.
38 Scott MG, Rosenberger CM, Gold MR, Finlay BB & Hancock RE (2000) An alpha-helical cationic antimicrobial peptide selectively modulates macrophage responses to lipopolysaccharide and directly alters macrophage gene expression. *J Immunol* **165**, 3358–3365.
39 Scott MG, Vreugdenhil AC, Buurman WA, Hancock RE & Gold MR (2000) Cutting edge: cationic antimicrobial peptides block the binding of lipopolysaccharide (LPS) to LPS binding protein. *J Immunol* **164**, 549–553.
40 Kounalakis NS & Corbett SA (2006) Lipopolysaccharide transiently activates THP-1 cell adhesion. *J Surg Res* **135**, 137–143.
41 Wieczorek M, Jenssen H, Kindrachuk J, Scott WR, Elliott M, Hilpert K, Cheng JT, Hancock RE & Straus SK (2010) Structural studies of a peptide with immune modulating and direct antimicrobial activity. *Chem Biol* **17**, 970–980.
42 Li FK, Davenport A, Robson RL, Loetscher P, Rothlein R, Williams JD & Topley N (1998) Leukocyte migration across human peritoneal mesothelial cells is dependent on directed chemokine secretion and ICAM-1 expression. *Kidney Int* **54**, 2170–2183.
43 Fenjves ES, Gordon DA, Pershing LK, Williams DL & Taichman LB (1989) Systemic distribution of apolipoprotein E secreted by grafts of epidermal keratinocytes: implications for epidermal function and gene therapy. *Proc Natl Acad Sci USA* **86**, 8803–8807.
44 Richmond JM & Harris JE (2014) Immunology and skin in health and disease. *Cold Spring Harb Perspect Med* **4**, a015339.
45 Papareddy P, Kalle M, Kasetty G, Mörgelin M, Rydengård V, Albiger B, Lundqvist K, Malmsten M & Schmidtchen A (2010) C-terminal peptides of tissue factor pathway inhibitor are novel host defense molecules. *J Biol Chem* **285**, 28387–28398.
46 Andersson E, Rydengard V, Sonesson A, Morgelin M, Bjorck L & Schmidtchen A (2004) Antimicrobial activities of heparin-binding peptides. *Eur J Biochem* **271**, 1219–1226.
47 Kok E, Haikonen S, Luoto T, Huhtala H, Goebeler S, Haapasalo H & Karhunen PJ (2009) Apolipoprotein E-dependent accumulation of Alzheimer disease-related lesions begins in middle age. *Ann Neurol* **65**, 650–657.
48 Nordahl EA, Rydengård V, Nyberg P, Nitsche DP, Mörgelin M, Malmsten M, Björck L & Schmidtchen A (2004) Activation of the complement system generates antibacterial peptides. *Proc Natl Acad Sci USA* **101**, 16879–16884.
49 Braesch-Andersen S, Paulie S, Smedman C, Mia S & Kumagai-Braesch M (2013) ApoE production in human monocytes and its regulation by inflammatory cytokines. *PLoS One* **8**, e79908.
50 Dobson CB, Sales SD, Hoggard P, Wozniak MA & Crutcher KA (2006) The receptor-binding region of human apolipoprotein E has direct anti-infective activity. *J Infect Dis* **193**, 442–450.
51 Li FQ, Fowler KA, Neil JE, Colton CA & Vitek MP (2010) An apolipoprotein E-mimetic stimulates axonal regeneration and remyelination after peripheral nerve injury. *J Pharmacol Exp Ther* **334**, 106–115.
52 Azevedo OG, Oliveira RA, Oliveira BC, Zaja-Milatovic S, Araújo CV, Wong DV, Costa TB, Lucena HB, Lima RC Jr, Ribeiro RA *et al.* (2012) Apolipoprotein E COG 133 mimetic peptide improves 5-fluorouracil-induced intestinal mucositis. *BMC Gastroenterol* **12**, 35.
53 Wiegand I, Hilpert K & Hancock RE (2008) Agar and broth dilution methods to determine the minimal inhibitory concentration (MIC) of antimicrobial substances. *Nat Protoc* **3**, 163–175.
54 Pizzo E, Merlino A, Turano M, Russo Krauss I, Coscia F, Zanfardino A, Varcamonti M, Furia A, Giancola C, Mazzarella L *et al.* (2011) A new RNase sheds light on the RNase/angiogenin subfamily from zebrafish. *Biochem J* **433**, 345–355.
55 Boukamp P, Popp S, Altmeyer S, Hülsen A, Fasching C, Cremer T & Fusenig NE (1997) Sustained non tumorigenic phenotype correlates with a largely stable chromosome content during long-term culture of the human keratinocyte line HaCaT. *Genes Chromosom Cancer* **19**, 201–214.
56 Livak KJ & Schmittgen TD (2001) Analysis of relative gene expression data using real-time quantitative PCR and the 2(-DeltaDelta C(T)) Method. *Methods* **25**, 402–408.
57 World Medical Organization (1996) Declaration of Helsinki. *Br Med J* **313**, 1448–1449.
58 Ke N, Wang X, Xu X & Abassi YA (2011) The xCELLigence system for real-time and label-free monitoring of cell viability. *Methods Mol Biol* **740**, 33–43.
59 Solly K, Wang X, Xu X, Strulovici B & Zheng W (2004) Application of real-time cell electronic sensing (RT-CES) technology to cell-based assays. *Assay Drug Dev Technol* **2**, 363–372.
60 Angstmann M, Brinkmann I, Bieback K, Breitkreutz D & Maercker C (2011) Monitoring human mesenchymal stromal cell differentiation by electrochemical impedance sensing. *Cytotherapy* **13**, 1074–1089.
61 Park HE, Kim D, Koh HS, Cho S, Sung JS & Kim JY (2011) Real-time monitoring of neural differentiation of human mesenchymal stem cells by electric cell-substrate impedance sensing. *J Biomed Biotechnol*, doi: 10.1155/2011/485173.